
000 001 002 003 004 005 006 007 008 009 010 011 012 013 014 015 016 017 018 019 020 021 022 023 024 025 026 027 028 029 030 031 032 033 034 035 036 037 038 039 040 041 042 043 044 045 046 047 048 049 050 051 052 053 COMPRESSION AWARE CERTIFIED TRAINING

Anonymous authors

Paper under double-blind review

ABSTRACT

Deep neural networks deployed in safety-critical, resource-constrained environments must balance efficiency and robustness. Existing methods treat compression and certified robustness as separate goals, compromising either efficiency or safety. We propose CACTUS (Compression Aware Certified Training Using network Sets), a general framework for unifying these objectives during training. CACTUS models maintain high certified accuracy even when compressed and generalize across multiple compression levels without retraining. We apply CACTUS for both pruning and quantization and show that it effectively trains models which can be efficiently compressed while maintaining high accuracy and certifiable robustness. CACTUS achieves state-of-the-art accuracy and certified performance for both pruning and quantization on a variety of datasets and input specifications.

1 INTRODUCTION

Deep neural networks (DNNs) are widely adopted in safety-critical applications such as autonomous driving Bojarski et al. (2016); Shafaei et al. (2018), medical diagnosis Amato et al. (2013); Kononenko (2001), and wireless systems Cho et al. (2023); Yang et al. (2018) due to their state-of-the-art accuracy. However, deploying these models in resource-constrained environments necessitates model compression to satisfy strict computational, memory, and latency requirements. Furthermore, using machine learning in safety-critical environments requires networks that are provably robust. Current compression methods, including pruning and quantization, effectively reduce model complexity but frequently degrade robustness, either by discarding essential features or amplifying adversarial vulnerabilities. Conversely, certified robust training methods Singh et al. (2018); Zhang et al. (2019); Mueller et al. (2022); Mao et al. (2023) predominantly target full-precision models and, as shown in our evaluation, lose substantial certified robustness under compression, resulting in a critical research gap: robustly trained models rarely consider compression, while compressed models rarely maintain robustness. In many real-world systems, both efficiency and reliability are non-negotiable.

Most existing approaches treat compression and robustness as independent objectives. Techniques for compression-aware training often overlook certifiable robustness, focusing primarily on reducing model size Zimmer et al. (2022). Similarly, methods that achieve certifiable robustness typically do not account for compression, leading to suboptimal standard and certified accuracy when models are compressed Vaishnavi et al. (2022). These limitations force practitioners to choose between deploying larger, resource-intensive models for robustness or sacrificing safety for efficiency. Furthermore, edge devices that leverage compressed networks often face evolving computational needs, necessitating adaptable models that can be efficiently compressed at multiple levels Francy & Singh (2024). Therefore, developing training methodologies that produce models adaptable to multi-level compression while maintaining certifiable robustness is crucial for optimal performance in dynamic, resource-constrained environments.

Is it possible to train neural networks that maintain **certified** robustness under **compression**?

Key Challenges. Integrating compression and certified robustness into a unified training framework presents unique challenges beyond simply combining existing loss functions. The fundamental difficulty lies in the competing nature of these objectives. Moreover, the compression space is vast

054 and discontinuous, making it non-trivial to select representative compression configurations that
055 effectively guide training. Additionally, common compression techniques use non-differentiable
056 operations (binary masks, rounding), requiring approximations that preserve theoretical guarantees.
057

058 **This work.** We propose CACTUS (Compression Aware Certified Training Using network Sets),
059 a novel framework that addresses these challenges through several key innovations. First, we de-
060 velop principled compression set selection strategies that balance computational cost with effective
061 coverage of the compression space, a non-trivial problem where larger sets do not always improve
062 performance. Second, we provide the first formal theoretical analysis connecting Adversarial Weight
063 Perturbation (AWP) to quantization robustness in the certified training context, establishing rigor-
064 ous foundations for our approach. Third, we demonstrate that joint training enables qualitatively
065 different model behaviors: CACTUS networks develop feature representations that naturally adapt
066 to compression, achieving certified robustness across multiple compression levels from a single
067 training run. Unlike sequential approaches that first train for robustness then compress, joint training
068 fundamentally changes the optimization landscape. Networks must develop internal representations
069 that are simultaneously robust to adversarial perturbations *and* resilient to compression artifacts.
070 This requires careful coordination and principled strategies for selecting compression configurations
071 during training. Naive combinations of existing techniques fail because they do not address these
072 fundamental optimization challenges.

073 **Main Contributions.** We list our main contributions below:
074

- 075 • We provide the first formal analysis connecting AWP to quantization robustness in certified training
076 (Theorem 4.1), establishing theoretical guarantees for our approximation scheme.
- 077 • We develop and analyze strategies for selecting compression configurations during training, showing
078 this is a non-trivial optimization problem where naive approaches lead to suboptimal performance.
- 079 • We propose CACTUS, a framework for training networks which with formal gaurantees under
080 compression. A general approach that enables networks to develop compression-aware robust rep-
081 resentations, achieving certified robustness across multiple compression levels without retraining.
- 082 • We demonstrate significant improvements over sequential baselines across diverse settings, showing
083 the benefits of joint optimization over post-hoc compression of robust models.

084 2 BACKGROUND

085 This section provides the necessary notations, definitions, and background on neural network com-
086 pression and certified training methods for DNNs.

087 **Notation.** Throughout the rest of the paper we use small case letters (x, y) for constants, bold
088 small case letters (\mathbf{x}, \mathbf{y}) for vectors, capital letters X, Y for functions and random variables, and
089 calligraphed capital letters \mathcal{X}, \mathcal{Y} for sets.

090 2.1 COMPRESSION OF NEURAL NETWORKS

091 Despite DNNs’ effectiveness, their high computational cost and memory footprint can hinder their
092 deployment on edge devices. To address these challenges, researchers have developed a variety of
093 compression strategies. In this paper, we will mainly focus on two of the more common strategies:
094 pruning and quantization. More details on both methods in Appendix A.

095 **Pruning.** Pruning is a widely adopted compression technique that reduces neural network size by
096 eliminating redundant weights or neurons, thereby decreasing memory usage and computational
097 cost. The lottery ticket hypothesis posits that within dense, randomly-initialized networks exist
098 sparse subnetworks—termed “winning tickets” that can be trained to be comparable to the original
099 network Frankle & Carbin (2019). Pruning methods are generally categorized based on: (1) unstruc-
100 tured pruning removes individual weights, while structured pruning eliminates entire structures like
101 neurons or filters; and (2) global pruning considers the entire network for pruning decisions, whereas
102 local pruning applies pruning within individual layers (3) whether they finetune after pruning or not
103 Cheng et al. (2024); Fladmark et al. (2023).

104 **Quantization.** Quantization is a prevalent technique for compressing neural networks by reducing the
105 bit-width of weights and activations, thereby decreasing memory usage and computational overhead.
106 By substituting high-precision floating-point representations (typically 32-bit) with lower-precision

108 formats, such as 8-bit integers, quantization can significantly accelerate inference, particularly on
109 hardware optimized for integer operations Wu et al. (2020b).

110 We denote the quantization operation as $Q : \mathbb{R} \times \mathbb{R}^+ \rightarrow \mathbb{R}$, which maps a weight w to its quantized
111 value with step size q_{step} . For a network f_θ parameterized by θ , we write $\theta^{Q,q_{step}}$ to denote the
112 quantized parameters where each $\theta_i^{Q,q_{step}} = Q(\theta_i, q_{step})$, and $f_\theta^{Q,q_{step}}$ to denote the network with
113 quantized parameters.

115 2.2 ADVERSARIAL ATTACKS, VERIFICATION, AND CERTIFIED TRAINING

116 Given an input-output pair $(\mathbf{x}, y) \in \mathcal{X} \subseteq \mathbb{R}^{d_{in}} \times \mathbb{Z}$, and a classifier $f : \mathbb{R}^{d_{in}} \rightarrow \mathbb{R}^{d_{out}}$ which is
117 parameterized by θ (written as f_θ). Let $\hat{f}(\mathbf{x}) = \arg \max_{k \in [d_{out}]} f(\mathbf{x})[k]$ be the predicted class of
118 \mathbf{x} . An additive perturbation, $\mathbf{v} \in \mathbb{R}^{d_{in}}$, is adversarial for f on \mathbf{x} if $\hat{f}(\mathbf{x}) = y$ and $\hat{f}(\mathbf{x} + \mathbf{v}) \neq y$.
119 Let $\mathcal{B}_p(\alpha, \beta) = \{\mathbf{x} \mid \|\mathbf{x} - \alpha\|_p \leq \beta\}$ be an l_p -norm ball. A classifier is adversarially robust on \mathbf{x}
120 for $\mathcal{B}_p(0, \epsilon)$ if it classifies all elements within the ball added to \mathbf{x} to the correct class. Formally,
121 $\forall \mathbf{v} \in \mathcal{B}_p(0, \epsilon). \hat{f}(\mathbf{x} + \mathbf{v}) = y$. In this paper, we focus on l_∞ -robustness, i.e. balls of the form
122 $\mathcal{B}_\infty(\mathbf{x}, \epsilon) := \{\mathbf{x}' = \mathbf{x} + \mathbf{v} \mid \|\mathbf{v}\|_\infty \leq \epsilon\}$, so will drop the subscript ∞ .

123 **Verification of NNs.** Given a neural network f_θ and an input \mathbf{x} with true label y , *certified robustness*
124 guarantees that the network's prediction remains unchanged for all inputs within a specified
125 perturbation bound $\mathcal{B}(\mathbf{x}, \epsilon)$. Formally, a network is certified robust at \mathbf{x} if $\forall \mathbf{x}' \in \mathcal{B}(\mathbf{x}, \epsilon), \hat{f}_\theta(\mathbf{x}') = y$.

126 Computing exact certified robustness is NP-hard for general neural networks. To address this,
127 researchers have developed various verification methods that provide sound and complete guarantees.
128 One popular approach is *Interval Bound Propagation* (IBP), which propagates interval bounds
129 through the network to compute sound over-approximations of the network's output range. While
130 IBP is computationally efficient, its bounds can be overly conservative. More precise methods like
131 $\alpha\beta$ -CROWN Wang et al. (2021) and DeepPoly Singh et al. (2019) exist but are more expensive.

132 **Training for Robustness.** We can get robustness by minimizing the expected worst-case loss due to
133 adversarial examples Mueller et al. (2022); Mao et al. (2023); Madry et al. (2018):

$$134 \theta = \arg \min_{\theta} \mathbb{E}_{(\mathbf{x}, y) \in \mathcal{X}} \left[\max_{\mathbf{x}' \in \mathcal{B}(\mathbf{x}, \epsilon)} \mathcal{L}(f_\theta(\mathbf{x}'), y) \right] \quad (1)$$

135 Where \mathcal{L} is a loss over the output of the DNN. Exactly solving the inner maximization is computa-
136 tionally intractable, in practice, it is approximated. Underapproximating the inner maximization is
137 typically called adversarial training, a popular technique for obtaining good empirical robustness
138 Madry et al. (2018), but these techniques do not give formal guarantees and are potentially vulnerable
139 to stronger attacks Tramer et al. (2020). We focus on certified training which overapproximates the
140 inner maximization as it provides better provable guarantees on robustness.

141 **Certified Training.** The IBP verification framework above adapts well to training. The BOX bounds
142 on the output can be encoded nicely into a loss function:

$$143 \mathcal{L}_{\text{IBP}}(\mathbf{x}, y, \epsilon) := \ln \left(1 + \sum_{i \neq y} e^{\bar{o}_i - \underline{o}_y} \right) \quad (2)$$

144 Where \bar{o}_i and \underline{o}_y represent the upper bound on output dimension i and lower bound of output
145 dimension y . To address the large approximation errors arising from BOX analysis, SABR Mueller
146 et al. (2022), a SOTA certified training method, obtains better standard and certified accuracy
147 by propagating smaller boxes through the network. They first compute an adversarial example,
148 $\mathbf{x}' \in \mathcal{B}(\mathbf{x}, \epsilon - \tau)$ in a slightly truncated l_∞ -norm ball. They then compute the IBP loss on a small
149 ball around the adversarial example, $\mathcal{B}(\mathbf{x}', \tau)$, rather than on the entire ball, $\mathcal{B}(\mathbf{x}, \epsilon)$, where $\tau \ll \epsilon$.

$$150 \mathcal{L}_{\text{SABR}}(\mathbf{x}, y, \epsilon, \tau) := \max_{\mathbf{x}' \in \mathcal{B}(\mathbf{x}, \epsilon - \tau)} \mathcal{L}_{\text{IBP}}(\mathbf{x}', y, \tau) \quad (3)$$

162 Although this is not a sound approximation, SABR accumulates fewer approximation errors due
163 to its more precise BOX analysis; thus, reduces overregularization and improves standard/certified
164 accuracy. Finally, we introduce Adversarial Weight Perturbation (AWP), a robust training method
165 which we use as a differentiable approximation from quantization, more details in Section 4.3.

166 **Adversarial Weight Perturbation.** AWP improves adversarial robustness by perturbing the weights
167 of a neural network during training Wu et al. (2020a). Formally, given a neural network f_θ with
168 parameters θ , AWP solves the following min-max optimization problem:
169

$$\min_{\theta} \mathbb{E}_{(\mathbf{x}, y)} \left[\max_{\|\delta\|_2 \leq \rho} \mathcal{L}(f_{\theta+\delta}(\mathbf{x}), y) \right] \quad (4)$$

170 where δ represents the adversarial perturbation to the weights, constrained within an l_2 -norm ball of
171 radius ρ , and \mathcal{L} is the loss function. The inner maximization finds the worst-case weight perturbation
172 that maximizes the loss, while the outer minimization trains the network to be robust against such
173 perturbations. This approach encourages the network to find flat loss landscapes with respect to
174 weight perturbations, which correlates with better generalization and robustness properties.
175

176 3 RELATED WORK

177 **Certified Training.** Shi et al. (2021); Mirman et al. (2018); Balunović & Vechev (2020); Zhang
178 et al. (2019) are well-known approaches for certified training of standard DNNs. More recent works
179 Mueller et al. (2022); Xiao et al. (2019); Fan & Li (2021) integrate adversarial and certified training
180 techniques to achieve state-of-the-art performance in both robustness and clean accuracy. De Palma
181 et al. (2023) show that expressive losses obtained via convex combinations of adversarial and IBP
182 loss gives state-of-the-art performance.

183 **Pruning.** LeCun et al. (1990); Hassibi & Stork (1993) pruned parameters based on their influence on
184 the loss (using second-order information). Han et al. (2015; 2016) iteratively pruned the smallest-
185 magnitude weights, the networks are then fine-tuned to recover accuracy. Huang et al. (2020) uses
186 regularizers that push weights to zero. Recent works like Frantar & Alistarh (2023) show that
187 GPT-scale transformers can be pruned to over 50% sparsity with negligible loss in performance.

188 **Pruning & Certified Training.** Zhangheng et al. (2022) investigates the effects of pruning on certified
189 robustness and propose a novel stability-based pruning method, NRSLoss, which significantly boosts
190 certified robustness. Sehwag et al. (2020) introduce HYDRA, a pruning framework which uses
191 empirical risk minimization problem guided by robust training goals.

192 **Quantization.** Hubara et al. (2016); Rastegari et al. (2016) show that using binary weights and
193 activations greatly reduces memory and compute at some cost to accuracy. Jacob et al. (2018)
194 introduced 8-bit integer weights and activations for improved accuracy retention.
195

196 **Quantization & Certified Training.** Lechner et al. (2023) introduce Quantization-Aware Interval
197 Bound Propagation (QA-IBP), a novel method for training and certifying the robustness of quantized
198 neural networks (QNNs). CACTUS does not assume specific quantization patterns rather it leverages
199 insights from adversarial weight perturbation Wu et al. (2020a) to generate networks with flatter loss
200 landscapes relative to the weight parametrization.

201 **Joint Compression and Robustness.** While CACTUS is the first framework for joint compression-
202 aware certified training, prior work has explored joint optimization for compression and empirical
203 robustness. Hoffmann et al. (2021) explore how different pruning techniques effect model robustness.
204 ATMC Gui et al. (2019) jointly optimizes for pruning, quantization, and adversarial robustness with
205 constrained optimization. ATMC learns networks with a predefined pruning and quantization technique
206 at a fixed compression level. CACTUS provides formal guarantees over a range of compression
207 techniques and levels to enable dynamic deployment.
208

209 4 CACTUS

210 In this section, we define a joint training objective for robustness and compression then introduce
211 CACTUS as a way to optimize this objective.
212

216 4.1 COMPRESSION AND ROBUSTNESS AWARE TRAINING OBJECTIVE
217

218 Equation 1 gives the robustness training objective. Given parameterization θ , classifier $f_\theta : \mathbb{R}^{d_{\text{in}}} \rightarrow$
219 $\mathbb{R}^{d_{\text{out}}}$ represents a DNN parameterized by θ , let the size of the DNN (number of parameters) be
220 $d_f = |\theta|$. Given a compression parameterization ψ , let $C_\psi^{f_\theta} : \mathbb{R}^{d_{\text{in}}} \rightarrow \mathbb{R}^{d_{\text{out}}}$ be a compressed model
221 derived from f_θ . For example, for pruning, we can have $\psi \in \{0, 1\}^{d_f}$ representing a binary mask
222 on θ , in other words, $C_\psi^{f_\theta} = f_\theta \odot \psi$ where \odot denotes element-wise multiplication of the parameters
223 θ and mask ψ . Given a compression level $\delta \in [0, 1)$, let Ψ_δ represent the set of all compression
224 parameterizations ψ that compress the model by δ . In our pruning example, $\frac{1}{d_f} \sum_{i=1}^{d_f} \psi_i = 1 - \delta$.
225 Note that by this definition, the network is uncompressed when $\delta = 0$. Given a maximum compression
226 ratio, δ_{max} , we can now define the compression and robustness aware training objective as finding θ
227 that minimizes
228

229
230
$$\theta = \arg \min_{\theta} \mathbb{E}_{\delta \in [0, \delta_{\text{max}}]} \left[\min_{\psi \in \Psi_\delta} \left(\mathbb{E}_{(\mathbf{x}, y) \in \mathcal{X}} \left[\max_{\mathbf{x}' \in \mathcal{B}(\mathbf{x}, \epsilon)} \mathcal{L}(C_\psi^{f_\theta}(\mathbf{x}'), y) \right] \right) \right] \quad (5)$$

231
232

233 Here, the inner minimization searches for the compressed network with given compression ratio,
234 δ , that gives the smallest expected loss over an adversarially attacked dataset. Combined together,
235 the objective function optimizes for the network parameterization θ , which retains the best expected
236 performance across all compression ratios while under attack. For a given compression ratio,
237 even without the robustness condition, directly solving this minimization problem to find the best
238 compressed network is computationally impractical. For pruning and quantization, the search space is
239 highly discontinuous and non-differentiable. Thus, in practice, existing compression methods either
240 use heuristic-based searching to find compressed networks or depend on hardware considerations (e.g.
241 floating-point precision support) to limit the search space substantially Palakonda et al. (2025); Wang
242 et al. (2019); Zandonati et al. (2023). While for certain compression methods like pruning we could
243 potentially optimize over the entire search space, this problem becomes computationally impractical.
244 Following this intuition, we limit our search space to $\mathcal{C}(f_\theta)$, a set of compressed networks (including
245 the full network). For example, $\mathcal{C}(f_\theta)$ could contain the full network, f_θ , and f_θ pruned by global
246 l_1 -pruning at $\delta = 0.7$. We can now modify the above optimization problem to,
247

248
$$\theta = \arg \min_{\theta} \frac{1}{|\mathcal{C}(f_\theta)|} \sum_{\psi_\delta \in \mathcal{C}(f_\theta)} \left(\mathbb{E}_{(\mathbf{x}, y) \in \mathcal{X}} \left[\max_{\mathbf{x}' \in \mathcal{B}(\mathbf{x}, \epsilon)} \mathcal{L}(C_{\psi_\delta}^{f_\theta}(\mathbf{x}'), y) \right] \right) \quad (6)$$

249
250

251 Recall that although solving Equation 1 exactly is computationally impractical, we can overap-
252 proximate the inner maximization using techniques like IBP Gowal et al. (2018) to create tractable
253 certifiably robust training algorithms. CACTUS overapproximates Equation 6 in a similar manner.
254

255 4.2 CACTUS LOSS
256

257 For a given network, $C_{\psi_\delta}^{f_\theta} \in \mathcal{C}(f_\theta)$, and data point, $\mathbf{x}, \mathbf{y} \in \mathcal{X}$, we can define the loss as
258

259
$$\lambda \mathcal{L}_{\text{std}}(C_{\psi_\delta}^{f_\theta}(\mathbf{x}), \mathbf{y}) + (1 - \lambda) \mathcal{L}_{\text{cert}}(C_{\psi_\delta}^{f_\theta}(\mathbf{x}), \mathbf{y}) \quad (7)$$

260

261 where $\lambda \in [0, 1]$ is a hyperparameter that balances the relative importance of standard accuracy versus
262 certified robustness. Rather than using a fixed λ throughout training, we employ a curriculum-based
263 approach where we initially train without the robust loss ($\lambda = 0$) and gradually increase λ up to 0.75
264 over the course of training. This progressive scaling allows the model to first establish stable feature
265 representations before introducing the challenging robust training objective, significantly improving
266 training stability and preventing competing gradients from robustness and compression objectives
267 from causing training instability.

268 Although CACTUS is general for different standard and certified loss functions. For the remainder of
269 this paper, we will be using cross-entropy for standard loss and SABR for certified loss (Equation 3).
CACTUS's development is orthogonal to general certified training techniques. Here, while we could

use IBP Shi et al. (2021) loss or losses due to more complicated abstract domains Singh et al. (2018; 2019) we leverage SABR’s insight that using smaller unsound IBP boxes around adversarial examples leads to less approximation errors during bound propagation and thus higher standard and certified accuracy. To overapproximate Equation 6, we can now define CACTUS loss as

$$\mathcal{L}_{CACTUS} = \frac{1}{|\mathcal{C}(f_\theta)|} \sum_{\psi_\delta \in \mathcal{C}(f_\theta)} \lambda \mathcal{L}_{std}(C_{\psi_\delta}^{f_\theta}(\mathbf{x}), \mathbf{y}) + (1 - \lambda) \mathcal{L}_{cert}(C_{\psi_\delta}^{f_\theta}(\mathbf{x}), \mathbf{y}) \quad (8)$$

Borrowing insight from existing works on certified training, we balance certified loss with standard loss Mueller et al. (2022); Mao et al. (2023); Shi et al. (2021). Here, we are assuming that we can propagate the gradient on $C_{\psi_\delta}^{f_\theta}$ back to f_θ . While for some compression techniques, such as pruning, this is possible, some compression algorithms (quantization) perform non-differentiable transforms (such as rounding). In the following sections, we show how we can use differentiable analogs to train.

4.3 CACTUS TRAINING

CACTUS training proceeds by jointly optimizing over a set of compressed network configurations $\mathcal{C}(f_\theta)$ during each training iteration. For each batch, the algorithm refreshes the compression set based on current weights, then computes both standard and certified losses for each compressed network, accumulating the weighted average as the final CACTUS loss. For pruning, gradients propagate directly through the subset of active weights, while quantization requires Adversarial Weight Perturbation (AWP) as a differentiable proxy. Our Theorem 4.1 establishes that AWP provides a sound upper bound for quantized network losses when the perturbation magnitude η exceeds the quantization step size, enabling principled joint optimization. The complete algorithm and detailed AWP analysis are provided in Appendix B. Since quantization is not differentiable, we use *adversarial weight perturbation* (AWP) Wu et al. (2020a) as a differentiable proxy for quantization.

Adversarial Weight Perturbation. When quantizing weights to a fixed-point format with step size q_{step} , the quantization error for each weight is bounded by $q_{step}/2$. This means the quantized weights lie within an l_∞ ball of radius $q_{step}/2$ around the original weights. AWP directly optimizes for robustness against such bounded perturbations. Thus, instead of applying a standard quantization step, we consider the worst-case perturbation to θ within a bounded neighborhood (l_∞ -norm less than η) that could degrade the final quantized parameters. Formally, for each training step, we solve

$$\Delta^* = \arg \max_{\{\Delta \mid \|\Delta\|_\infty \leq \eta\}} \mathcal{L}_{std}(f_{\theta+\Delta}(x), y) + \mathcal{L}_{cert}(f_{\theta+\Delta}(x), y) \quad (9)$$

where η defines the magnitude of allowable weight perturbations. This objective can be approximated efficiently via gradient ascent. The resulting Δ^* provides a worst-case perturbation that exposes vulnerabilities in the quantization mapping. We then update both θ in the direction that lowers this worst-case loss, thereby making the model more robust to shifts that might arise from discretizing the parameters. More formally, we have

Theorem 4.1. *Given network f_θ , loss functions \mathcal{L}_{std} , \mathcal{L}_{cert} , perturbation magnitude η and Δ^* computed by Equation 9. If $q_{step} \leq 2\eta$, then*

$$\mathcal{L}_{std}(f_{\theta+\Delta^*}(x), y) + \mathcal{L}_{cert}(f_{\theta+\Delta^*}(x), y) \geq \mathcal{L}_{std}(f_\theta^{Q, q_{step}}(x), y) + \mathcal{L}_{cert}(f_\theta^{Q, q_{step}}(x), y)$$

Proof Sketch. If $q_{step} \leq 2\eta$ then $\exists \Delta' \in \{\Delta \mid \|\Delta\|_\infty \leq \eta\}$ s.t. $f_{\theta+\Delta'} = f_\theta^{Q, q_{step}}$, In other words, as long as η is sufficiently large, training with AWP covers the quantization. Full proof in Appendix D.

Theorem 4.1 provides the key practical insight that AWP can serve as a differentiable proxy for quantization in certified training. In practice, we compute an approximate Δ^* using a gradient-based approach; however, our experimental results show that we still get good performance.

4.4 COMPRESSION SET SELECTION STRATEGIES

The choice of compression set $\mathcal{C}(f_\theta)$ is crucial for CACTUS’s performance. We propose and analyze several strategies:

324	325	Dataset	Model	ϵ	Pruning	HYDRA		NRSLoss		Pruning	SABR		CACTUS	
						Amount	Std.	Cert.	Std.	Cert.	Method	Std.	Cert.	Std.
326	327	MNIST	CNN7	0.1	0	98.56	98.13	98.98	98.13	-	99.23	98.22	99.15	97.98
328	329				0.5	98.55	97.21	98.45	97.82	GSl_2	97.62	95.09	98.73	97.16
330	331				0.7	96.37	95.14	97.62	96.21	LUL_1	98.71	93.88	98.75	95.39
332	333			0.3	0	96.28	92.88	95.15	91.15	GSl_2	94.85	95.73	97.96	96.02
334	335				0.5	93.12	91.76	95.16	90.25	LUL_1	95.11	87.68	97.83	95.61
336	337				0.7	94.02	88.25	95.10	90.67	GSl_2	94.32	86.61	97.96	91.87
338	339	CIFAR-10	CNN7	$\frac{2}{255}$	0	72.88	61.45	75.27	61.26	-	79.21	62.83	78.29	61.90
340	341				0.5	73.46	62.16	76.14	61.24	GSl_2	76.32	56.87	78.03	62.57
342	343				0.7	76.32	61.29	76.25	61.88	LUL_1	78.14	58.08	79.13	63.16
344	345			$\frac{8}{255}$	0	45.38	29.12	50.25	30.44	GSl_2	71.62	54.92	76.37	61.63
346	347				0.5	44.65	31.27	48.29	30.48	LUL_1	73.31	57.27	79.30	64.74
348	349				0.7	45.89	26.31	47.16	30.56	GSl_2	46.20	22.38	50.76	30.41
350	351									LUL_1	49.96	31.73	51.94	32.46

Table 1: Standard and Certified Accuracy for MNIST ($\epsilon = 0.1, 0.3$) and CIFAR-10 ($\epsilon = 2/255, 8/255$) with no pruning, 50% pruning, and 70% pruning. CACTUS is compared to HYDRA, NRSLoss, and SABR. HYDRA and NRSLoss are custom pruning methods. For CACTUS and SABR we use global structured l_2 -pruning (GSl_2) and local unstructured l_1 -pruning (LUL_1)

1. **Fixed Sparsity Levels:** For pruning, we can include networks pruned at fixed sparsity levels (e.g., 25%, 50%, 75%). This provides a systematic coverage of the compression space.
2. **Sampling:** At each iteration, instead of training on all networks in the compression set, we can take the full network and randomly sample another network from the set to train on.
3. **Progressive Compression:** We can start with a small compression set and gradually increase its size during training, allowing the model to adapt to increasing compression levels.

We study this choice in Appendix F. We find that sampling a fixed set provides a good balance between performance and computational efficiency. The relationship between the compression set size and performance is non-monotonic as larger compression sets don't necessarily lead to better performance, as shown in our experiments below.

5 EVALUATION

We compare CACTUS to existing pruning (HYDRA Sehwag et al. (2020), NRSLoss Zhangcheng et al. (2022)) and quantization (QA-IBP Lechner et al. (2023)) methods which focus on optimizing both certified training and compression. We also compare against SABR Mueller et al. (2022) a state-of-the-art certified training method (that does not consider compression).

Experimental Setup. All experiments were performed on an A100-80Gb. We use $\alpha\beta$ -CROWN Wang et al. (2021), a state-of-the-art complete verifier for neural networks, to compute certified accuracy with a 300 second timeout per input. We consider two popular image recognition datasets: MNIST Deng (2012) and CIFAR10 Krizhevsky et al. (2009). We use a variety of challenging l_∞ perturbation bounds common in verification/robust training literature Xu et al. (2021); Wang et al. (2021); Singh et al. (2019; 2018); Shi et al. (2021); Mueller et al. (2022); Mao et al. (2023). We use a 7-layer convolutional architecture, CNN7, used in many prior works we compare against Shi et al. (2021); Mueller et al. (2022); Mao et al. (2023). Results are given averaged over the test sets for each dataset. See Appendix C for more details.

378	379	Dataset	Model	ϵ	Quantization	QA-IBP		SABR		CACTUS			
						Std.	Cert.	Std.	Cert.	Std.	Cert.		
380	381	MNIST	CNN7	0.1	-	99.02	98.34	99.23	98.22	99.15	98.16		
382	383				fp16	-	-	96.14	81.12	98.89	97.33		
384	385				int8	99.12	95.21	93.45	56.14	98.45	95.62		
386	387				-	97.25	92.13	98.75	93.40	98.14	92.89		
388	389			0.3	fp16	-	-	96.24	74.28	97.98	92.55		
390	391				int8	95.67	91.24	88.25	15.23	96.07	92.01		
392	393				-	71.25	58.26	79.21	62.83	75.78	60.73		
394	395				$\frac{2}{255}$	fp16	-	67.18	31.25	74.65	58.27		
396	CIFAR-10	CNN7			int8	64.47	56.90	68.28	17.86	71.24	58.33		
397					-	36.78	22.53	52.38	35.13	51.27	32.65		
398		$\frac{8}{255}$		fp16	-	-	45.35	12.11	48.16	31.89			
399				int8	32.57	20.75	42.18	1.12	49.38	28.81			

Table 2: Standard and Certified Accuracy for MNIST ($\epsilon = 0.1, 0.3$) and CIFAR-10 ($\epsilon = 2/255, 8/255$) with no, fp16, and int8 quantization. CACTUS is compared to QA-IBP and SABR.

We evaluate CACTUS on standard image datasets, attack budgets, and compression ratios. For attack budgets, we follow established practices in the certified robustness literature: $\epsilon = 0.1, 0.3$ for MNIST and $\epsilon = 2/255, 8/255$ for CIFAR-10. These values represent realistic threat models while remaining computationally tractable for verification. For pruning amounts, we use on $[0.25, 0.5, 0.75]$ for training and $[0, 0.5, 0.7]$ for testing as these values represent a practical trade-off between model size reduction and performance retention. While higher pruning ratios (up to 99%) are also popular Piras et al. (2024), we focus on this range as it provides a good balance between compression and maintaining certified robustness, in Appendix F we present results for pruning ratios $[0.9, 0.95, 0.99]$. In Appendix F, we also provide runtime results, errorbars, results on TinyImagenet and additional model architectures, study on choice of compression set, additional bit-widths for quantization, and joint vs. sequential training. Additional details can be found in Appendix C.

5.1 MAIN RESULTS

Pruning. We perform a best-effort reproduction of both HYDRA Sehwag et al. (2020) and NRSLoss Zhangheng et al. (2022) using SABR as the pretrained network for both. We use the settings as described in the respective papers. For CACTUS, we set $\mathcal{C}(f_\theta)$ to be the full unpruned network and a network pruned with global unstructured l_1 with δ chosen uniformly from $[0.25, 0.5, 0.75]$. Table 1 gives these results for MNIST at $\epsilon = 0.1, 0.3$ and for CIFAR-10 at $\epsilon = 2/255, 8/255$ comparing results at $\delta = [0, 0.5, 0.7]$. To show CACTUS’s generality we use two unseen pruning methods GSl_2 (global structured l_2) and LUL_1 (local unstructured l_1). When unpruned ($\delta = 0$), SABR itself achieves the best performance for both standard and certified accuracy, which is by design: CACTUS is optimized for certified accuracy under compression rather than uncompressed performance. Given CACTUS’s increased optimization complexity from jointly optimizing for compression and robustness, it achieves on-par performance with SABR while uncompressed. At all pruning levels, CACTUS has the best performance for both standard and certified accuracy aside from one instance (NRSLoss has better certified accuracy at MNIST, $\epsilon = 0.1, \delta = 0.7$ but even in this case CACTUS is close obtaining 96.02 vs. 96.21). The results also show that CACTUS generalizes well even to unseen pruning methods as its performance is relatively stable between the two methods.

Quantization. We perform a best-effort reproduction of QA-IBP Lechner et al. (2023) for CNN7 using the settings provided in the paper. QA-IBP was implemented with 8-bit integer quantization so we give results for QA-IBP unquantized and quantized to int8. CACTUS is trained with AWP radius, η , to 0.25. We quantize CACTUS and SABR to both fp16 and int8. Results can be seen in Table 2. Like pruning, we see that CACTUS beats both baselines in almost all compressed benchmarks (aside from MNIST, $\epsilon = 0.1$, int8 where QA-IBP gets better standard accuracy 99.12 vs 98.45). CACTUS obtains especially good results for harder problems, we see that for CIFAR-10 8/255 CACTUS obtains 7.2% better standard and and 8.06% better certified accuracy compared to baselines.

432 5.2 FURTHER EXPERIMENTS/ABLATIONS
433

434 **Runtime Analysis.** CACTUS training takes 33-40% more time than SABR training. While CACTUS
435 incurs additional overhead due to training over multiple compressed network configurations, this
436 one-time cost is justified by significant performance improvements and could be reduced through
437 optimizations like caching compressed models (see Appendix E for details).

438 **Memory Overhead.** CACTUS requires additional memory during training to maintain activations
439 for multiple models in the compression set. For CNN7 on CIFAR-10 with batch size 32, we measure
440 SABR consuming 12.8 GB of GPU memory while CACTUS consumes 23.7 GB (representing an
441 85% increase).

442 **Integration with Additional Certified Training Methods.** For the remainder of our experiments
443 we use CIFAR-10, $\epsilon = 8/255$. CACTUS is in parallel with certified training methods and
444 can incorporate any certified training approach as its base loss function \mathcal{L}_{cert} . To demonstrate this
445 flexibility and show that CACTUS's improvements extend beyond our choice of SABR as the baseline
446 certified training method, we integrate CACTUS with recent state-of-the-art certified training methods
447 from CTBENCH Mao et al. (2024). Table 3 shows results on CIFAR-10 with $\epsilon = 8/255$ for both
448 quantization and pruning scenarios, comparing standalone certified training methods against their
449 integration within the CACTUS framework.

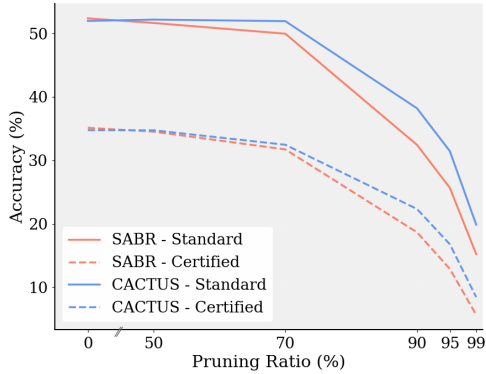
450

Method	Quantization (int8)		Pruning (0.7 $LU\ell_1$)	
	Clean Acc	Cert Acc	Clean Acc	Cert Acc
SABR	42.2	1.1	50.0	31.7
TAPS	41.8	1.1	49.5	30.9
STAPS	43.4	0.9	51.2	28.4
MTL-IBP	44.2	2.1	49.6	31.9
CACTUS+SABR	49.4	28.8	51.9	32.5
CACTUS+TAPS	48.9	28.9	52.7	33.3
CACTUS+MTL-IBP	49.1	29.2	52.5	33.7

461 Table 3: Comparison of certified training methods and their integration with CACTUS
462

463 The results demonstrate two key findings. First, standalone certified training methods (SABR, TAPS,
464 STAPS, MTL-IBP) achieve minimal certified accuracy under compression, with the best performing
465 method (MTL-IBP) reaching only 2.1% certified accuracy under int8 quantization. Second, integrating
466 these same methods within the CACTUS framework consistently yields substantial improvements
467 across all base methods and compression scenarios. This demonstrates that CACTUS's benefits arise
468 from the joint optimization approach rather than the specific choice of certified training baseline.

469 The consistent improvements across different base certified training methods validate our meta-
470 framework design and show that CACTUS's compression-aware training strategies can enhance any
471 underlying certified training approach. This flexibility makes CACTUS broadly applicable as the
472 certified training field continues to evolve with new methods.

473 **Extreme Sparsity Performance.** Figure 1
474 shows CACTUS versus SABR certified ac-
475 curacy across a wide range of sparsity lev-
476 els [0, 0.5, 0.7, 0.9, 0.95, 0.99] for CIFAR-10
477 with $\epsilon = 8/255$. The results demonstrate three
478 key findings: (1) CACTUS maintains its ad-
479 vantage over SABR even at extreme sparsity
480 levels, (2) both methods degrade gracefully
481 until approximately 0.95 sparsity then drop
482 sharply, and (3) CACTUS's relative improve-
483 ment increases with compression level, high-
484 lighting the benefits of compression-aware
485 training for aggressive compression scen-
486 arios. Detailed results for these extreme sparsity
487 levels are provided in Appendix F.

487 Figure 1: Performance of CACTUS and SABR on
488 CIFAR-10 as a function of sparsity.

486
487 **Varying AWP radius.** When training CACTUS for quantization we use AWP Wu et al. (2020a) as a
488 differentiable approximation for quantization. When computing the worst-case adversarial weight
489 perturbation, we must choose a maximum perturbation budget, η , for the attack such that the l_∞ -norm
490 of the perturbation is within η . In Table 4, we compare different choices of η . We observe that
491 higher values of η result in more stable results after pruning but generally lead to lower standard and
492 certified accuracy when uncompressed. Conversely, when choosing small η while the uncompressed
493 model performs well, after quantization this performance drops quickly. We choose $\eta = 0.25$ as it
494 obtains good quantization results (only losing to $\eta = 0.5$ for fp16 but only by 0.08) while maintaining
495 relatively high uncompressed performance.

		Quant. Metric	$\eta = 0.1$	$\eta = 0.25$	$\eta = 0.5$	$\eta = 1$
497 -	Std.	53.47	51.27	50.87	21.25	
	Cert.	36.27	32.65	28.50	15.42	
498 fp16	Std.	45.17	48.16	48.24	20.45	
	Cert.	28.45	31.89	28.14	16.72	
500 int8	Std.	42.36	49.38	46.29	19.66	
	Cert.	16.72	28.81	27.86	15.89	

504
505 Table 4: Exploring different values of η . Models
506 are trained using AWP with each value of η then
507 evaluated on fp16 and int8.

	Comp.	Metric	Pruned Mdl	Quant. Mdl	Both
None	Std.	51.97	51.27	50.11	
	Cert.	34.76	32.65	31.87	
0.7	Std.	51.94	45.62	48.63	
	Cert.	32.46	27.94	31.20	
int8	Std.	38.16	49.16	42.62	
	Cert.	21.64	28.81	27.51	

504
505 Table 5: Pruned model from Table 1. Quant. model
506 from Table 2. Both models jointly optimize over
507 quantization and pruning.

508 **Pruning and Quantization.** CACTUS does not restrict us from simultaneously training to optimize
509 for both pruning and quantization. If we directly use both our AWP approximation for quantization and
510 a pruned model when training we get standard and certified accuracies of 50.11 and 31.87 respectively.
511 Table 5 gives results for pruning and quantization objectives. While the model trained on both does
512 not perform as well as each individual model, it strikes a balance obtaining good performance for both.
513 We believe that joint optimization for both pruning and quantization is inherently more difficult than
514 optimizing for either alone. Networks optimized for pruning prefer concentrated capacity in a smaller
515 number of ‘important’ weights, allowing them to maintain performance with sparse connectivity. In
516 contrast, networks optimized for quantization prefer weights clustered around quantization levels to
517 minimize discretization error. Simultaneously considering both objectives significantly increases the
518 optimization complexity, as the network must find a compromise that satisfies both constraints while
519 maintaining accuracy and robustness.

520 6 CONCLUSION

521 We present CACTUS, a framework that unifies certified robustness and model compression during
522 training. By co-optimizing over adversarial perturbations and compression-induced architectural/numerical
523 perturbations, CACTUS ensures models remain provably robust even when pruned or
524 quantized. Our method generalizes across compression levels, enabling a single model to adapt
525 dynamically to varying edge-device constraints without retraining. Experiments demonstrate CACTUS
526 maintains accuracy and certified robustness of non-compressed baselines under a variety of
527 compression ratios across multiple datasets. We detail CACTUS’s limitations in Appendix G. This work
528 bridges a critical gap in deploying safe, efficient AI systems in resource-constrained environments.

531 7 ETHICS & REPRODUCIBILITY STATEMENT

532 The authors affirm adherence to the ICLR Code of Ethics throughout the research and submission
533 process. We have made extensive efforts to ensure the reproducibility of our results and encourage
534 replication of our work. Complete proofs for all theoretical claims, including Theorem 4.1, are
535 provided in Appendix D. All mathematical assumptions and derivations are clearly stated. Compre-
536 hensive experimental details are provided in Appendix C, including network architectures, training
537 hyperparameters, hardware specifications, and dataset preprocessing steps. Specific training con-
538 figurations for CACTUS, including compression set selection strategies and λ scheduling, are fully
539 documented. Detailed algorithmic descriptions are provided in Appendix B, including the complete

540 CACTUS training procedure and adversarial weight perturbation implementation details. All hy-
541 perparameters used in our experiments are explicitly listed. All datasets used in our experiments
542 (MNIST, CIFAR-10, TinyImageNet) are publicly available. Source code for reproducing our results
543 will be made available upon acceptance to facilitate replication and extension of this work.

544 **Use of Large Language Models.** Large language models (LLMs) were used in a limited capacity to
545 assist with writing and editing tasks.

547 **REFERENCES**

549 Filippo Amato, Alberto López, Eladia María Peña-Méndez, Petr Vaňhara, Aleš Hampl, and Josef
550 Havel. Artificial neural networks in medical diagnosis. *Journal of Applied Biomedicine*, 11(2),
551 2013.

552 Mislav Balunović and Martin Vechev. Adversarial training and provable defenses: Bridging the gap.
553 In *8th International Conference on Learning Representations (ICLR 2020)(virtual)*. International
554 Conference on Learning Representations, 2020.

556 Mariusz Bojarski, Davide Del Testa, Daniel Dworakowski, Bernhard Firner, Beat Flepp, Prasoon
557 Goyal, Lawrence D Jackel, Mathew Monfort, Urs Muller, Jiakai Zhang, et al. End to end learning
558 for self-driving cars. *arXiv preprint arXiv:1604.07316*, 2016.

559 Gregory Bonaert, Dimitar I Dimitrov, Maximilian Baader, and Martin Vechev. Fast and precise
560 certification of transformers. In *Proceedings of the 42nd ACM SIGPLAN international conference*
561 *on programming language design and implementation*, pp. 466–481, 2021.

562 Hongrong Cheng, Miao Zhang, and Javen Qinfeng Shi. A survey on deep neural network pruning:
563 Taxonomy, comparison, analysis, and recommendations. *IEEE Transactions on Pattern Analysis*
564 *and Machine Intelligence*, 46(12):10558–10578, 2024. doi: 10.1109/TPAMI.2024.3447085.

566 Kun Woo Cho, Marco Cominelli, Francesco Gringoli, Joerg Widmer, and Kyle Jamieson. Scalable
567 multi-modal learning for cross-link channel prediction in massive iot networks. In *Proceedings of*
568 *the Twenty-Fourth International Symposium on Theory, Algorithmic Foundations, and Protocol*
569 *Design for Mobile Networks and Mobile Computing*. MobiHoc '23, pp. 221–229, New York, NY,
570 USA, 2023. Association for Computing Machinery. ISBN 9781450399265. doi: 10.1145/3565287.
571 3610280. URL <https://doi.org/10.1145/3565287.3610280>.

572 Alessandro De Palma, Rudy Bunel, Krishnamurthy Dvijotham, M Pawan Kumar, Robert Stanforth,
573 and Alessio Lomuscio. Expressive losses for verified robustness via convex combinations. *arXiv*
574 *preprint arXiv:2305.13991*, 2023.

575 Li Deng. The mnist database of handwritten digit images for machine learning research. *IEEE Signal*
576 *Processing Magazine*, 29(6):141–142, 2012.

578 Jiameng Fan and Wenchao Li. Adversarial training and provable robustness: A tale of two objectives.
579 In *Proceedings of the AAAI Conference on Artificial Intelligence*, volume 35, pp. 7367–7376, 2021.

580 Eirik Fladmark, Muhammad Hamza Sajjad, and Laura Brinkholm Justesen. Exploring the perfor-
581 mance of pruning methods in neural networks: An empirical study of the lottery ticket hypothesis,
582 2023. URL <https://arxiv.org/abs/2303.15479>.

584 Samer Francy and Raghbir Singh. Edge ai: Evaluation of model compression techniques for
585 convolutional neural networks, 2024. URL <https://arxiv.org/abs/2409.02134>.

586 Jonathan Frankle and Michael Carbin. The lottery ticket hypothesis: Finding sparse, trainable neural
587 networks, 2019. URL <https://arxiv.org/abs/1803.03635>.

588 Elias Frantar and Dan Alistarh. Sparsegpt: massive language models can be accurately pruned in
589 one-shot. In *Proceedings of the 40th International Conference on Machine Learning*, ICML'23.
590 JMLR.org, 2023.

592 Sven Gowal, Krishnamurthy Dvijotham, Robert Stanforth, Rudy Bunel, Chongli Qin, Jonathan
593 Uesato, Relja Arandjelovic, Timothy Mann, and Pushmeet Kohli. On the effectiveness of interval
bound propagation for training verifiably robust models. *arXiv e-prints*, pp. arXiv–1810, 2018.

594 Shupeng Gui, Haotao Wang, Haichuan Yang, Chen Yu, Zhangyang Wang, and Ji Liu. Model
595 compression with adversarial robustness: A unified optimization framework. *Advances in neural*
596 *information processing systems*, 32, 2019.

597 Song Han, Jeff Pool, John Tran, and William J. Dally. Learning both weights and connections
598 for efficient neural networks. In *Proceedings of the 29th International Conference on Neural*
599 *Information Processing Systems - Volume 1*, NIPS'15, pp. 1135–1143, Cambridge, MA, USA,
600 2015. MIT Press.

602 Song Han, Huiyi Mao, and William J. Dally. Deep compression: Compressing deep neural network
603 with pruning, trained quantization and huffman coding. In Yoshua Bengio and Yann LeCun (eds.),
604 *4th International Conference on Learning Representations, ICLR 2016, San Juan, Puerto Rico,*
605 *May 2-4, 2016, Conference Track Proceedings*, 2016. URL <http://arxiv.org/abs/1510.00149>.

607 Babak Hassibi and David G. Stork. Second order derivatives for network pruning: Optimal brain
608 surgeon. In *Advances in Neural Information Processing Systems (NeurIPS)*, volume 6, pp. 164–171,
609 1993.

610 Jasper Hoffmann, Shashank Agnihotri, Tonmoy Saikia, and Thomas Brox. Towards improving
611 robustness of compressed cnns. In *ICML Workshop on Uncertainty and Robustness in Deep*
612 *Learning (UDL)*, 2021.

614 Chang-Ti Huang, Jun-Cheng Chen, and Ja-Ling Wu. Learning sparse neural networks through
615 mixture-distributed regularization. In *2020 IEEE/CVF Conference on Computer Vision and Pattern*
616 *Recognition Workshops (CVPRW)*, pp. 2968–2977, 2020. doi: 10.1109/CVPRW50498.2020.00355.

617 Itay Hubara, Matthieu Courbariaux, Daniel Soudry, Ran El-Yaniv, and Yoshua Bengio. Binarized
618 neural networks. In *Proceedings of the 30th International Conference on Neural Information*
619 *Processing Systems*, NIPS'16, pp. 4114–4122, Red Hook, NY, USA, 2016. Curran Associates Inc.
620 ISBN 9781510838819.

621 Sergey Ioffe and Christian Szegedy. Batch normalization: accelerating deep network training
622 by reducing internal covariate shift. In *Proceedings of the 32nd International Conference on*
623 *International Conference on Machine Learning - Volume 37*, ICML'15, pp. 448–456. JMLR.org,
624 2015.

626 Benoit Jacob, Skirmantas Kligys, Bo Chen, Menglong Zhu, Matthew Tang, Andrew Howard, Hartwig
627 Adam, and Dmitry Kalenichenko. Quantization and training of neural networks for efficient
628 integer-arithmetic-only inference. In *Proceedings of the IEEE Conference on Computer Vision and*
629 *Pattern Recognition (CVPR)*, June 2018.

630 Igor Kononenko. Machine learning for medical diagnosis: history, state of the art and perspective.
631 *Artificial Intelligence in medicine*, 23(1):89–109, 2001.

632 Alex Krizhevsky, Geoffrey Hinton, et al. Learning multiple layers of features from tiny images, 2009.

634 Mathias Lechner, DJordje Žikelić, Krishnendu Chatterjee, Thomas A Henzinger, and Daniela Rus.
635 Quantization-aware interval bound propagation for training certifiably robust quantized neural
636 networks. In *Proceedings of the AAAI Conference on Artificial Intelligence*, volume 37, pp.
637 14964–14973, 2023.

638 Yann LeCun, John S. Denker, and Sara A. Solla. Optimal brain damage. In *Advances in Neural*
639 *Information Processing Systems (NeurIPS)*, volume 2, pp. 598–605, 1990.

641 Qun Li, Yuan Meng, Chen Tang, Jiacheng Jiang, and Zhi Wang. Investigating the impact of
642 quantization on adversarial robustness. *arXiv preprint arXiv:2404.05639*, 2024.

643 Aleksander Madry, Aleksandar Makelov, Ludwig Schmidt, Dimitris Tsipras, and Adrian Vladu.
644 Towards deep learning models resistant to adversarial attacks. In *International Conference on*
645 *Learning Representations*, 2018.

647 Yuhao Mao, Mark Niklas Müller, Marc Fischer, and Martin Vechev. Taps: Connecting certified and
adversarial training. *arXiv e-prints*, pp. arXiv–2305, 2023.

648 Yuhao Mao, Stefan Balaucă, and Martin Vechev. Ctbench: A library and benchmark for certified
649 training. *arXiv preprint arXiv:2406.04848*, 2024.

650

651 Matthew Mirman, Timon Gehr, and Martin Vechev. Differentiable abstract interpretation for provably
652 robust neural networks. In *International Conference on Machine Learning*, pp. 3578–3586. PMLR,
653 2018.

654 Mark Niklas Mueller, Franziska Eckert, Marc Fischer, and Martin Vechev. Certified training: Small
655 boxes are all you need. In *The Eleventh International Conference on Learning Representations*,
656 2022.

657

658 Vikas Palakonda, Jamshid Tursunboev, Jae-Mo Kang, and Sunghwan Moon. Metaheuristics for prun-
659 ing convolutional neural networks: A comparative study. *Expert Systems with Applications*, 268:
660 126326, 2025. ISSN 0957-4174. doi: <https://doi.org/10.1016/j.eswa.2024.126326>. URL <https://www.sciencedirect.com/science/article/pii/S0957417424031932>.

661

662 Adam Paszke, Sam Gross, Francisco Massa, Adam Lerer, James Bradbury, Gregory Chanan, Trevor
663 Killeen, Zeming Lin, Natalia Gimelshein, Luca Antiga, et al. Pytorch: An imperative style,
664 high-performance deep learning library. *Advances in neural information processing systems*, 32,
665 2019.

666

667 Giorgio Piras, Maura Pintor, Ambra Demontis, Battista Biggio, Giorgio Giacinto, and Fabio Roli.
668 Adversarial pruning: A survey and benchmark of pruning methods for adversarial robustness, 2024.
669 URL <https://arxiv.org/abs/2409.01249>.

670

671 Mohammad Rastegari, Vicente Ordonez, Joseph Redmon, and Ali Farhadi. Xnor-net: Imagenet
672 classification using binary convolutional neural networks. In Bastian Leibe, Jiri Matas, Nicu Sebe,
673 and Max Welling (eds.), *Computer Vision – ECCV 2016*, pp. 525–542, Cham, 2016. Springer
674 International Publishing. ISBN 978-3-319-46493-0.

675

676 Vikash Sehwag, Shiqi Wang, Prateek Mittal, and Suman Jana. Hydra: Pruning adversarially robust
677 neural networks. *Advances in Neural Information Processing Systems*, 33:19655–19666, 2020.

678

679 Sina Shafaei, Stefan Kugel, Mohd Hafeez Osman, and Alois Knoll. Uncertainty in machine learning:
680 A safety perspective on autonomous driving. In *Computer Safety, Reliability, and Security: SAFECOMP 2018 Workshops, ASSURE, DECSoS, SASSUR, STRIVE, and WAISE, Västerås,
681 Sweden, September 18, 2018, Proceedings 37*, pp. 458–464. Springer, 2018.

682

683 Zhouxing Shi, Huan Zhang, Kai-Wei Chang, Minlie Huang, and Cho-Jui Hsieh. Robustness verifica-
684 tion for transformers. *arXiv preprint arXiv:2002.06622*, 2020.

685

686 Zhouxing Shi, Yihan Wang, Huan Zhang, Jinfeng Yi, and Cho-Jui Hsieh. Fast certified robust training
687 with short warmup. *Advances in Neural Information Processing Systems*, 34:18335–18349, 2021.

688

689 Gagandeep Singh, Timon Gehr, Matthew Mirman, Markus Püschel, and Martin Vechev. Fast and
690 effective robustness certification. *Advances in neural information processing systems*, 31, 2018.

691

692 Gagandeep Singh, Timon Gehr, Markus Püschel, and Martin Vechev. An abstract domain for
693 certifying neural networks. *Proceedings of the ACM on Programming Languages*, 3(POPL):1–30,
694 2019.

695

696 Florian Tramer, Nicholas Carlini, Wieland Brendel, and Aleksander Madry. On adaptive attacks to
697 adversarial example defenses. *Advances in neural information processing systems*, 33:1633–1645,
698 2020.

699

700 Pratik Vaishnavi, Veena Krish, Farhan Ahmed, Kevin Eykholt, and Amir Rahmati. On the feasibility
701 of compressing certifiably robust neural networks. In *Proceedings of the Third Workshop on
Trustworthy Machine Learning in OpenReview*, 2022.

702

703 Matthew Wallace, Rishabh Khandelwal, and Brian Tang. Does ibp scale? *bjaytang.com*, 2022.

704

705 Kuan Wang, Zhijian Liu, Yujun Lin, Ji Lin, and Song Han. Haq: Hardware-aware automated
706 quantization with mixed precision. In *2019 IEEE/CVF Conference on Computer Vision and Pattern
707 Recognition (CVPR)*, pp. 8604–8612, 2019. doi: 10.1109/CVPR.2019.00881.

702 Shiqi Wang, Huan Zhang, Kaidi Xu, Xue Lin, Suman Jana, Cho-Jui Hsieh, and J Zico Kolter.
703 Beta-CROWN: Efficient bound propagation with per-neuron split constraints for complete and
704 incomplete neural network verification. *Advances in Neural Information Processing Systems*, 34,
705 2021.

706 Dongxian Wu, Shu-Tao Xia, and Yisen Wang. Adversarial weight perturbation helps robust general-
707 ization. *Advances in neural information processing systems*, 33:2958–2969, 2020a.

709 Hao Wu, Patrick Judd, Xiaojie Zhang, Mikhail Isaev, and Paulius Micikevicius. Integer quantization
710 for deep learning inference: Principles and empirical evaluation, 2020b. URL <https://arxiv.org/abs/2004.09602>.

712 Kai Y. Xiao, Vincent Tjeng, Nur Muhammad (Mahi) Shafullah, and Aleksander Madry. Training
713 for faster adversarial robustness verification via inducing reLU stability. In *International Confer-
714 ence on Learning Representations*, 2019. URL <https://openreview.net/forum?id=BJfIVjAcKm>.

716 Kaidi Xu, Huan Zhang, Shiqi Wang, Yihan Wang, Suman Jana, Xue Lin, and Cho-Jui Hsieh. Fast
717 and Complete: Enabling complete neural network verification with rapid and massively parallel
718 incomplete verifiers. In *International Conference on Learning Representations*, 2021. URL
719 <https://openreview.net/forum?id=nVZtXB16LNn>.

721 Chao Yang, Xuyu Wang, and Shiwen Mao. Autotag: Recurrent variational autoencoder for un-
722 supervised apnea detection with rfid tags. In *2018 IEEE Global Communications Conference
723 (GLOBECOM)*, pp. 1–7, 2018. doi: 10.1109/GLOCOM.2018.8648073.

724 Ben Zandonati, Glenn Bucagu, Adrian Alan Pol, Maurizio Pierini, Olya Sirkin, and Tal Kopetz.
725 Towards optimal compression: Joint pruning and quantization, 2023. URL <https://arxiv.org/abs/2302.07612>.

728 Huan Zhang, Hongge Chen, Chaowei Xiao, Bo Li, Duane Boning, and Cho-Jui Hsieh. Towards
729 stable and efficient training of verifiably robust neural networks. *arXiv preprint arXiv:1906.06316*,
730 2019.

731 LI Zhangheng, Tianlong Chen, Linyi Li, Bo Li, and Zhangyang Wang. Can pruning improve certified
732 robustness of neural networks? *Transactions on Machine Learning Research*, 2022.

734 Max Zimmer, Christoph Spiegel, and Sebastian Pokutta. Compression-aware training of neural
735 networks using frank-wolfe. *arXiv preprint arXiv:2205.11921*, 2022.

736

737

738

739

740

741

742

743

744

745

746

747

748

749

750

751

752

753

754

755

756

757

758

759

760

761

762

Appendix

Table of Contents

A	Extended Background	15
764	A.1 Detailed Compression Methods	15
765		
B	CACTUS Training Algorithm	16
767	B.1 Complete Training Procedure	16
768		
C	Experimental Details	17
770	C.1 Implementation Details	17
771	C.2 λ Schedule Justification	17
772	C.3 Network Architectures	18
773		
D	Proofs	18
774	D.1 Proof of Theorem 4.1	18
775		
E	Runtime Analysis	19
777	E.1 Computational Overhead	19
778	E.2 Memory Efficiency	19
779		
F	Further Experiments	20
781	F.1 Scaling to Larger Architectures	20
782	F.2 Statistical Significance	20
783	F.3 Exploring Set Selection	20
784	F.4 Comprehensive Compression Set Selection Analysis	21
785	F.5 High Sparsity Results	22
786	F.6 Additional Model Architectures	22
787	F.7 TinyImageNet Results	22
788	F.8 Extended Bit-width Evaluation	23
789	F.9 Joint vs. Sequential Training	23
790		
G	Limitations	23

791

792

793

794

A EXTENDED BACKGROUND

795

796

A.1 DETAILED COMPRESSION METHODS

797

798

A.1.1 PRUNING METHODS

799

800

Pruning methods can be categorized along several dimensions. We provide a detailed taxonomy here:

801

802

Magnitude-based Pruning. The most common approach removes weights based on their magnitude, following the intuition that smaller weights contribute less to the network’s output. For a weight tensor W , we define a pruning mask M such that:

803

804

805

$$M_{ij} = \begin{cases} 1 & \text{if } |W_{ij}| > t \\ 0 & \text{otherwise} \end{cases} \quad (10)$$

806

where t is a threshold determined by the desired sparsity ratio.

807

808

809

Global vs. Local Pruning. Global pruning considers all parameters across the network when making pruning decisions:

$$t_{global} = \text{percentile}(\{|W_{ij}| : \forall i, j, l\}, (1 - s) \times 100\%) \quad (11)$$

810 where s is the target sparsity ratio and l indexes layers.
 811
 812 Local pruning applies pruning independently to each layer:
 813
 814
 815
$$t_{local}^{(l)} = \text{percentile}(\{|W_{ij}^{(l)}| : \forall i, j\}, (1 - s) \times 100\%) \quad (12)$$

 816
 817

818 **Structured vs. Unstructured Pruning.** Unstructured pruning removes individual weights, leading
 819 to sparse connectivity patterns. Structured pruning removes entire channels, filters, or neurons,
 820 maintaining dense subnetworks that are more hardware-friendly.

821 For channel pruning, we remove entire channels based on importance scores. Common importance
 822 metrics include: - l_1 -norm: $\text{score}_c = \|W_{:,c,:,:}\|_1$ - l_2 -norm: $\text{score}_c = \|W_{:,c,:,:}\|_2$ - Gradient-based:
 823 $\text{score}_c = \|\nabla_W L \odot W_{:,c,:,:}\|_2$

824
 825
 826 **A.1.2 QUANTIZATION METHODS**
 827

828 **Post-Training Quantization (PTQ).** PTQ quantizes a pre-trained floating-point model. For uniform
 829 quantization, the quantization function is:
 830

831
 832
$$Q(w) = \text{clamp}\left(\left\lfloor \frac{w - z}{s} \right\rfloor, q_{min}, q_{max}\right) \cdot s + z \quad (13)$$

 833
 834

835 where s is the scale factor, z is the zero point, and q_{min}, q_{max} define the quantization range.
 836

837 **Quantization-Aware Training (QAT).** QAT simulates quantization during training using the straight-
 838 through estimator (STE):
 839

840
 841
$$\frac{\partial Q(w)}{\partial w} \approx \begin{cases} 1 & \text{if } q_{min} \leq \frac{w - z}{s} \leq q_{max} \\ 0 & \text{otherwise} \end{cases} \quad (14)$$

 842
 843

844 The scale and zero-point parameters are typically learned or computed based on weight statistics:
 845

846
 847
$$s = \frac{\max(w) - \min(w)}{q_{max} - q_{min}}, \quad z = q_{min} - \frac{\min(w)}{s} \quad (15)$$

 848
 849

850
 851 **B CACTUS TRAINING ALGORITHM**
 852

853 This section provides the complete CACTUS training algorithm and detailed analysis of our Adver-
 854 sarial Weight Perturbation approach for quantization.
 855

856
 857 **B.1 COMPLETE TRAINING PROCEDURE**
 858

859
 860 Algorithm 1 outlines CACTUS’s procedure for co-optimizing compression and robustness. At each
 861 iteration, the algorithm samples a batch of training data, generates compressed networks, computes
 862 the standard and certified loss on each compressed network, and finally updates θ .
 863

864 **Algorithm 1** CACTUS Training
 865 **Require:** Training data \mathcal{X} , compression set $\mathcal{C}(f_\theta)$, robustness radius ϵ , loss weights λ
 866 1: Initialize θ
 867 2: **for** each training iteration $t = 1, 2, \dots, T$ **do**
 868 3: **for** each batch $(\mathbf{x}, \mathbf{y}) \subset \mathcal{X}$ **do**
 869 4: Refresh $\mathcal{C}(f_\theta)$ for current θ :
 870 5: For pruning: Update pruning masks based on current weights
 871 6: For quantization: Update quantization levels based on weight distributions
 872 7: $\mathcal{L}_{CACTUS} = 0$
 873 8: **for** $\psi_\theta \in \mathcal{C}(f_\theta)$ **do**
 874 9: Compute compressed network $C_{\psi_\theta}^{f_\theta}$
 875 10: Calculate \mathcal{L}_{std} and \mathcal{L}_{cert}
 876 11: $\mathcal{L}_{CACTUS} += \frac{1}{|\mathcal{C}(f_\theta)|} [\lambda \mathcal{L}_{std} + (1 - \lambda) \mathcal{L}_{cert}]$
 877 12: Update θ
 878 13: **end for**
 879 14: **end for**
 880 15: **end for**
 881 16: **return** θ

882
 883
 884 During each batch in Algorithm 1 it is important to refresh the compressed networks to ensure that
 885 gradient updates can be accurately propagated (i.e. compressed networks are recomputed). Once
 886 refreshed, for pruning, we can directly propagate gradient updates back to the original network as the
 887 pruned network weights are a subset of the entire network.

888
 889 **C** EXPERIMENTAL DETAILS
 890

891 **C.1** IMPLEMENTATION DETAILS
 892

893 We implemented CACTUS in PyTorch Paszke et al. (2019). All networks are trained using the Adam
 894 optimizer with a learning rate of $1e - 4$ and weight decay $1e - 5$. All networks are trained with 100
 895 epochs. We use a batch size of 16 for MNIST and 32 for CIFAR-10. Sticking with standard IBP
 896 protocols, we start by warming up with standard loss for the first 250 iterations (250 batches). For
 897 the next 250 batches we linearly scale λ from 0 to 0.75 then remain constant for the remainder of
 898 training.
 899

900 **C.2** λ SCHEDULE JUSTIFICATION
 901

902 We conducted hyperparameter searches to determine the optimal λ schedule and upper bound using
 903 CIFAR-10 with $\epsilon = 8/255$ under 0.7 global unstructured pruning. Our investigation revealed that
 904 directly applying $\lambda = 0.75$ from the beginning causes training instability, particularly when combined
 905 with compression objectives. A gradual increase enables the network to first learn basic features
 906 before incorporating robustness constraints—a critical consideration for CACTUS, which balances
 907 multiple competing objectives. We present comprehensive ablation studies below.
 908

909 **C.2.1** ABLATION 1: λ SCHEDULE SHAPE
 910

911 We evaluate three scheduling strategies, each reaching $\lambda_{max} = 0.75$:

912 The constant schedule performs poorly on both metrics, exhibiting training instability as the network
 913 struggles to simultaneously learn features and satisfy robustness constraints. The direct linear
 914 schedule achieves the highest standard accuracy (51.8%) but yields lower certified accuracy (26.1%).
 915 Our warmup + linear + constant approach achieves a modest 1% reduction in standard accuracy while
 916 providing a substantial 4.3% gain in certified accuracy (30.4%). Since CACTUS targets certified
 917 robustness under compression, this trade-off is favorable.

Schedule Strategy	Description	Standard Acc.	Certified Acc.
Constant	$\lambda = 0.75$ throughout training	35.6%	18.3%
Direct Linear	Linearly increase from 0 to 0.75	51.8%	26.1%
Warmup + Linear + Constant (Ours)	warmup ($\lambda = 0$), linear scaling (0→0.75), constant (0.75)	50.8%	30.4%

Table 6: Comparison of different λ scheduling strategies on CIFAR-10 with $\epsilon = 8/255$ under 0.7 global unstructured pruning.

C.2.2 ABLATION 2: λ_{max} UPPER BOUND

Using our warmup + linear + constant schedule, we ablate different maximum values for λ :

λ_{max}	Standard Acc.	Certified Acc.
0.25	52.0%	10.8%
0.50	51.7%	23.4%
0.75 (Ours)	50.8%	30.4%
1.00	38.9%	28.7%

Table 7: Ablation study on λ_{max} values using the warmup + linear + constant schedule on CIFAR-10 with $\epsilon = 8/255$ under 0.7 global unstructured pruning.

The results reveal a clear trade-off between standard and certified accuracy. As λ_{max} increases from 0.25 to 0.75, standard accuracy decreases gradually (47.1% → 45.8%) while certified accuracy improves substantially (10.8% → 30.4%). At $\lambda_{max} = 0.75$, we achieve the best certified accuracy with only a modest 1.3% reduction in standard accuracy compared to $\lambda_{max} = 0.25$. Beyond 0.75, at $\lambda_{max} = 1.00$, both metrics degrade significantly; we hypothesize this is due to the extreme emphasis on certified robustness impairing standard accuracy. This demonstrates that $\lambda_{max} = 0.75$ strikes the optimal balance, maximizing certified robustness without over-constraining the network.

While we acknowledge that this represents a subset of possible λ schedules and upper bounds, these hyperparameters achieve state-of-the-art performance. Further optimization remains an avenue for future work.

C.3 NETWORK ARCHITECTURES

C.3.1 CNN7 ARCHITECTURE

Similar to prior work Shi et al. (2021), we consider a 7-layer convolutional architecture, CNN7. The first 5 layers are convolutional layers with filter sizes [64, 64, 128, 128, 128], kernel size 3, strides [1, 1, 2, 1, 1], and padding 1. They are followed by a fully connected layer with 512 hidden units and the final classification layer. All but the last layers are followed by batch normalization Ioffe & Szegedy (2015) and ReLU activations. For the BN layers, we train using the statistics of the unperturbed data similar to Shi et al. (2021). During PGD attacks we use the BN layers in evaluation mode.

D PROOFS

D.1 PROOF OF THEOREM 4.1

Theorem D.1 (AWP Quantization Approximation). *Given network f_θ , loss functions \mathcal{L}_{std} , $\mathcal{L}_{\text{cert}}$, perturbation magnitude η and Δ computed by Equation 9. If $q_{step} \leq 2\eta$, then*

$$\mathcal{L}_{\text{std}}(f_{\theta+\Delta}(x), y) + \mathcal{L}_{\text{cert}}(f_{\theta+\Delta}(x), y) \geq \mathcal{L}_{\text{std}}(f_\theta^{Q, q_{step}}(x), y) + \mathcal{L}_{\text{cert}}(f_\theta^{Q, q_{step}}(x), y)$$

972 *Proof.* Let θ^Q denote the quantized parameters, i.e., $\theta^{Q,q_{step}} = Q(\theta, q_{step})$. By definition of uniform
973 quantization with step size q_{step} , each quantized weight satisfies:
974

$$975 \quad \theta_i^{Q,q_{step}} = q_{step} \cdot \left\lfloor \frac{\theta_i}{q_{step}} + 0.5 \right\rfloor \quad (16)$$

977 This means that for each parameter θ_i , the quantization error is bounded by:
978

$$979 \quad |\theta_i^{Q,q_{step}} - \theta_i| \leq \frac{q_{step}}{2} \quad (17)$$

981 Therefore, we have:
982

$$983 \quad \|\theta^{Q,q_{step}} - \theta\|_\infty \leq \frac{q_{step}}{2} \quad (18)$$

985 If $q_{step} \leq 2\eta$, then $\frac{q_{step}}{2} \leq \eta$, which means:
986

$$987 \quad \|\theta^{Q,q_{step}} - \theta\|_\infty \leq \eta \quad (19)$$

988 This implies that $\Delta' = \theta^{Q,q_{step}} - \theta$ satisfies the constraint $\|\Delta'\|_\infty \leq \eta$ in the AWP optimization
989 problem:
990

$$991 \quad \Delta^* = \arg \max_{\{\Delta \mid \|\Delta\|_\infty \leq \eta\}} \mathcal{L}_{\text{std}}(f_{\theta+\Delta}(x), y) + \mathcal{L}_{\text{cert}}(f_{\theta+\Delta}(x), y) \quad (20)$$

993 Since Δ^* is the optimal solution to this maximization problem and Δ' is a feasible point, we have:
994

$$995 \quad \mathcal{L}_{\text{std}}(f_{\theta+\Delta^*}(x), y) + \mathcal{L}_{\text{cert}}(f_{\theta+\Delta^*}(x), y) \quad (21)$$

$$996 \quad \geq \mathcal{L}_{\text{std}}(f_{\theta+\Delta'}(x), y) + \mathcal{L}_{\text{cert}}(f_{\theta+\Delta'}(x), y) \quad (22)$$

$$997 \quad = \mathcal{L}_{\text{std}}(f_{\theta}^{Q,q_{step}}(x), y) + \mathcal{L}_{\text{cert}}(f_{\theta}^{Q,q_{step}}(x), y) \quad (23)$$

1000 This completes the proof. □
1001

1003 E RUNTIME ANALYSIS

1005 CACTUS requires compression to be calculated at each batch increasing the cost of training. For
1006 CIFAR10 and $\epsilon = 8/255$, SABR training took 296 minutes, CACTUS training took 416 minutes
1007 for pruning and 365 minutes for quantization. QA-IBP took 312 minutes. While CACTUS takes
1008 longer than baselines we note that for most applications extra training time is worth the increased
1009 performance. We also note that CACTUS's training time could likely be optimized. For example, by
1010 caching and reusing compressed models for multiple batches before recomputing the overhead could
1011 be reduced. However, we leave such optimizations for future work. Both HYDRA and NRSLoss
1012 are pruning methods taking pretrained models so they cannot be fairly compared to CACTUS for
1013 runtime.

1014 E.1 COMPUTATIONAL OVERHEAD

1016 CACTUS incurs additional computational cost due to training over multiple compressed network
1017 configurations. However, this overhead is justified by the significant performance improvements and
1018 the fact that a single CACTUS model generalizes to various compression levels without retraining.
1019 The 33-40% increase in computational resources compared to standard certified training represents a
1020 one-time cost that is amortized across multiple deployment scenarios.

1022 E.2 MEMORY EFFICIENCY

1024 For large networks where memory is a constraint, CACTUS's loss can be computed for each network
1025 in $\mathcal{C}(f_\theta)$ separately using gradient accumulation, resulting in no additional memory utilization com-
pared to standard certified training. This makes the approach practical for large-scale deployments.

1026

F FURTHER EXPERIMENTS

1027

1028

F.1 SCALING TO LARGER ARCHITECTURES

1029

1030 CACTUS’s scalability is supported by existing work showing that certified training and verification
1031 scale to transformer networks Shi et al. (2020); Bonaert et al. (2021); Wallace et al. (2022). We
1032 demonstrate preliminary results on MobileViT architecture for CIFAR-10, achieving standard accu-
1033 racy of 45.2% under no compression and 41.8% under int8 quantization, with certified accuracies
1034 of 16.8% and 12.5% respectively. These results suggest that CACTUS can extend to larger, more
1035 complex architectures while maintaining its effectiveness.

1037

F.2 STATISTICAL SIGNIFICANCE

1039

1040 All reported results are averaged over 3 independent runs with different random seeds. We report
1041 mean values in the main tables. Standard deviations are provided in Table 8 below:

1042

Dataset	Method	Compression	Std. Acc. (\pm std)	Cert. Acc. (\pm std)
CIFAR-10	SABR	0	52.38 ± 0.82	35.13 ± 0.94
	CACTUS	0	51.97 ± 0.71	34.76 ± 0.89
	SABR	0.5	51.65 ± 0.94	34.52 ± 1.12
	CACTUS	0.5	52.18 ± 0.68	34.74 ± 0.95
	SABR	0.7	49.96 ± 1.15	31.73 ± 1.24
	CACTUS	0.7	51.94 ± 0.87	32.46 ± 1.08

1051 Table 8: Standard deviations for key results on CIFAR-10 with $\epsilon = 8/255$.

1053 The results show that CACTUS’s improvements are consistent across runs, with standard deviations
1054 comparable to baseline methods, indicating that the improvements are not due to random variance.

1057

F.3 EXPLORING SET SELECTION

1059

1060

	Prune	Metric	$\mathcal{U}(0.25, 0.75)$	$\mathcal{U}(0.25, 0.75)^3$	[0.25, 0.5, 0.75]
0	Std.	51.97	51.42	51.12	
	Cert.	34.76	35.13	34.62	
0.5	Std.	52.18	52.61	51.98	
	Cert.	34.74	34.69	34.54	
0.7	Std.	51.94	51.63	51.31	
	Cert.	32.46	33.21	32.10	

1069 Table 9: Exploring larger $\mathcal{C}(f_\theta)$ sets using LUL_1 . Here \mathcal{U} is a uniform distribution where \mathcal{U}^3 means
1070 that for each batch we sample three random δ s to prune with. The final set [0.25, 0.5, 0.75] represents
1071 three fixed values for δ .

1072 **Larger $\mathcal{C}(f_\theta)$ sets.** In Section 4.3, we discuss using a set $\mathcal{C}(f_\theta)$ comprised of the uncompressed
1073 network and a single (potentially randomly chosen) compressed network. However, CACTUS also
1074 allows us to optimize over multiple compressed networks. Recall that we currently set $\mathcal{C}(f_\theta)$ to be the
1075 full unpruned network and a network pruned with global unstructured l_1 while picking δ uniformly
1076 from $[0.25, 0.75]$. We can instead try using multiple randomly chosen δ for pruning or using a set
1077 list of δ s. Table F.3 gives the results for a single random δ , 3 random δ s, and a fixed set of δ s. We
1078 observe that the results are relatively constant between these three choices and thus since pruning
1079 more models adds computation time, we choose to use a single random δ .

1080 F.4 COMPREHENSIVE COMPRESSION SET SELECTION ANALYSIS
1081

1082 To thoroughly justify our compression set design choices, we conduct extensive experiments comparing
1083 different selection strategies across multiple dimensions: performance, computational efficiency,
1084 and coverage of the compression space.

1085 F.4.1 STRATEGY COMPARISON
1086

1087 We compare five different compression set selection strategies:
1088

Strategy	Training Time (min)	70% Pruned Std.	70% Pruned Cert.
Ours: $\mathcal{U}(0.25, 0.75)$	416	51.94	32.46
Fixed: $[0.25, 0.5, 0.75]$	623	51.31	32.10
Progressive: $0.25 \rightarrow 0.75$	587	51.67	32.34
Dense Sampling: 5 levels	1124	51.89	32.51
Adaptive: Top-k pruning	734	51.78	32.29

1097 Table 10: Comprehensive comparison of compression set selection strategies on CIFAR-10, $\epsilon =$
1098 $8/255$. Our random sampling approach achieves competitive performance across all metrics while
1099 requiring significantly less computational overhead.
1100

1101 **Strategy Details:**
1102

- **Ours ($\mathcal{U}(0.25, 0.75)$)**: Full network + one randomly sampled pruned network per batch
- **Fixed ($[0.25, 0.5, 0.75]$)**: Full network + three fixed pruning ratios
- **Progressive ($0.25 \rightarrow 0.75$)**: Start with 25% pruning, gradually increase to 75% over training epochs
- **Dense Sampling**: Full network + 5 uniformly spaced pruning levels $[0.15, 0.3, 0.45, 0.6, 0.75]$
- **Adaptive (Top-k)**: Full network + pruning levels selected based on weight magnitude distribution

1112 While our random sampling strategy does not achieve the highest performance in every metric, it
1113 provides competitive results across all measures while offering substantial computational savings.
1114 Specifically, it achieves within 0.6% standard accuracy and 0.05% certified accuracy of the best
1115 performing methods while requiring 33-63% less training time.
1116

1117 F.4.2 PERFORMANCE VS. COMPUTATIONAL COST TRADE-OFF
1118

1119 We analyze the trade-off between performance and computational overhead:
1120

Strategy	Set Size	Uncompressed		50% Pruned		70% Pruned	
		Std.	Cert.	Std.	Cert.	Std.	Cert.
Baseline (SABR)	1	51.65	34.52	49.96	31.73	47.23	28.89
CACTUS (Size 2)	2	51.97	34.76	52.18	34.74	51.94	32.46
CACTUS (Size 3)	3	51.42	35.13	52.61	34.69	51.63	33.21
CACTUS (Size 5)	5	51.23	34.89	52.34	34.45	51.78	32.67
CACTUS (Size 7)	7	50.89	34.67	51.89	34.12	51.45	32.34

1128 Table 11: Performance scaling with compression set size using uniform random sampling from
1129 $[0.2, 0.8]$.
1130

1131 While larger compression sets (size 3-5) can achieve slightly higher performance in some cases,
1132 the improvements are marginal (typically $\pm 1\%$) while computational cost increases substantially.
1133 Our choice of set size 2 provides an efficient balance, achieving competitive performance with
significantly reduced training overhead.

1134 F.5 HIGH SPARSITY RESULTS
1135

1136 We evaluate CACTUS’s performance at extreme pruning ratios to understand its behavior under
1137 aggressive compression:

1138

Dataset	ϵ	Prune Ratio	SABR		CACTUS		Improvement	
			Std.	Cert.	Std.	Cert.	Std.	Cert.
CIFAR-10	0.9	32.45	18.67	38.21	22.34	+5.76	+3.67	
	$\frac{8}{255}$	0.95	25.67	12.89	31.45	16.78	+5.78	+3.89
	0.99	15.23	5.67	19.87	8.45	+4.64	+2.78	
	0.9	45.32	32.45	48.67	35.23	+3.35	+2.78	
	$\frac{2}{255}$	0.95	38.45	26.78	42.34	29.56	+3.89	+2.78
	0.99	24.56	15.67	28.34	18.45	+3.78	+2.78	

1148 Table 12: Performance at high pruning ratios (0.9, 0.95, 0.99) showing CACTUS maintains advantages
1149 even under extreme compression.

1150 Even at very high pruning ratios (99% of weights removed), CACTUS maintains significant improvements
1151 over SABR, demonstrating the robustness of the approach across compression regimes.

1154 F.6 ADDITIONAL MODEL ARCHITECTURES

1155 We evaluate CACTUS on additional architectures to demonstrate generalizability, for the architectures
1156 and TinyImageNet we use α -crown Xu et al. (2021) as complete verification methods do not scale to
1157 larger networks/tinyimagenet well:

1159 F.6.1 RESNET-18 RESULTS

1160

Dataset	ϵ	Compression	SABR		CACTUS		Improvement	
			Std.	Cert.	Std.	Cert.	Std.	Cert.
CIFAR-10	$\frac{8}{255}$	0.5 Prune	45.32	28.76	48.65	31.24	+3.33	+2.48
		0.7 Prune	42.18	25.63	46.89	29.87	+4.71	+4.24
	$\frac{2}{255}$	fp16	62.45	45.32	65.78	48.67	+3.33	+3.35
		int8	58.67	41.23	62.34	44.78	+3.67	+3.55

1161 Table 13: ResNet-18 results on CIFAR-10 showing consistent improvements across architectures.

1172 F.7 TINYIMAGENET RESULTS

1173 To demonstrate scalability to larger datasets, we evaluate on TinyImageNet (200 classes, 64x64
1174 images):

1175

ϵ	Compression	SABR		CACTUS		Improvement	
		Std.	Cert.	Std.	Cert.	Std.	Cert.
$\frac{4}{255}$	None	32.45	18.67	31.78	18.23	-0.67	-0.44
	0.5 Prune	28.67	15.34	31.23	17.45	+2.56	+2.11
	0.7 Prune	25.45	12.78	28.67	15.23	+3.22	+2.45
	int8	29.34	16.45	30.78	17.34	+1.44	+0.89

1184 Table 14: TinyImageNet results using ResNet-18 architecture.

1185 On TinyImageNet, CACTUS shows consistent improvements for compressed networks, though the
1186 base performance is comparable. This suggests CACTUS’s benefits are most pronounced when
1187 compression significantly impacts performance.

1188 F.8 EXTENDED BIT-WIDTH EVALUATION
1189

1190 . To demonstrate CACTUS’s effectiveness across a broader range of quantization levels, we extend our
1191 evaluation to include more aggressive compression scenarios. Table 15 shows CACTUS performance
1192 on CIFAR-10 with $\epsilon = 8/255$ across different bit-widths including ultra-low precision quantization.
1193

Method	Clean Acc (%)	Certified Acc (%)
Full Precision	51.3	32.7
CACTUS (int8)	49.4	28.8
CACTUS (int6)	48.6	25.4
CACTUS (int4)	41.2	24.8
CACTUS (int2)	28.7	18.5

1201 Table 15: CACTUS performance across different quantization bit-widths on CIFAR-10 with $\epsilon =$
1202 $8/255$.
1203

1204 The results show that CACTUS maintains competitive performance even at extreme quantization
1205 levels, highlighting the effectiveness of our joint training approach for ultra-low precision scenarios.
1206 Even at int2 quantization, CACTUS retains substantial certified accuracy (18.5%), demonstrating its
1207 robustness to aggressive compression.
1208

1209 F.9 JOINT VS. SEQUENTIAL TRAINING 1210

1211 To demonstrate the effectiveness of joint optimization over sequential approaches, we compare CAC-
1212 TUS against sequential training baselines where we first train SABR to achieve certified robustness,
1213 then apply either Post-Training Quantization (PTQ) or Quantization-Aware Training (QAT). PTQ
1214 directly quantizes the trained robust model without additional training, while QAT fine-tunes the
1215 robust model with quantization simulation. We use the same PTQ and QAT setup from Li et al.
1216 (2024). Table 16 shows the results on CIFAR-10 with $\epsilon = 8/255$ and int8 quantization.
1217

Method	Clean Acc (%)	Certified Acc (%)	Training Time (min)
SABR→PTQ (int8)	43.6	4.6	312
SABR→QAT (int8)	48.2	9.3	345
CACTUS (int8)	49.4	28.8	416

1222 Table 16: Comparison of joint training (CACTUS) vs. sequential training approaches on CIFAR-10
1223 with $\epsilon = 8/255$ and int8 quantization.
1224

1225 While PTQ and QAT improve SABR’s original results, they fail to reach the level of CACTUS. We
1226 believe this is due to the difficulty of maintaining certified accuracy compared to empirical robustness.
1227 Joint training allows features to co-adapt to both adversarial perturbations and compression artifacts
1228 simultaneously, leading to significantly better performance under compression. While CACTUS
1229 incurs additional computational overhead compared to sequential approaches, this represents a one-
1230 time training cost that yields significant long-term benefits through superior generalization across
1231 compression levels.
1232

1233 G LIMITATIONS 1234

1235 While CACTUS successfully bridges compression and certified robustness training, our current
1236 implementation involves several design choices that present opportunities for future enhancement.
1237 For computational efficiency, we employ relatively small compression sets during training, though
1238 our experiments demonstrate that this constraint does not significantly impact the robustness benefits
1239 observed across compressed networks. The method does require additional computational resources
1240 during training (40-140% increase) as it processes multiple network variants simultaneously, repre-
1241 senting a reasonable trade-off for the substantial robustness gains achieved in compressed models.
1242 Our theoretical framework relies on standard assumptions common in robust optimization (uniform
1243

1242 quantization, Lipschitz continuity, ϵ -covering), and our current evaluation focuses on magnitude-
1243 based pruning and uniform quantization—established compression techniques that cover a significant
1244 portion of practical use cases. Our current evaluation is limited to the vision domain and small/mid
1245 sized datasets (MNIST, CIFAR-10, TinyImageNet). While these are standard datasets for certified
1246 training works we acknowledge our current evaluation is limited. CACTUS’s contributions are
1247 in parallel with advances in certified training, i.e. as certified training methods get stronger and
1248 scale to larger networks this allows CACTUS to scale to larger datasets as well. While the stan-
1249 dard and certified accuracy of full (uncompressed) networks trained with CACTUS do not exceed
1250 those of existing specialized methods optimized solely for uncompressed networks, this is expected
1251 given our focus on compression-robustness co-optimization. The approach represents a principled
1252 first step toward unified compression-aware robust training, with clear pathways for extending to
1253 larger compression sets, additional compression techniques, and hardware-specific optimizations as
1254 computational resources and theoretical understanding continue to advance.
1255
1256
1257
1258
1259
1260
1261
1262
1263
1264
1265
1266
1267
1268
1269
1270
1271
1272
1273
1274
1275
1276
1277
1278
1279
1280
1281
1282
1283
1284
1285
1286
1287
1288
1289
1290
1291
1292
1293
1294
1295